Supplementary Information: Photorealistic modelling of metals from first principles

Gianluca Prandini,[1] Gian-Marco Rignanese,[2] and Nicola Marzari[1,*]

[1] *Theory and Simulation of Materials (THEOS) and National Centre for Computational Design and Discovery of Novel Materials (MARVEL), École Polytechnique Fédérale de Lausanne, 1015 Lausanne, Switzerland*

[2] *Institute of Condensed Matter and Nanosciences (IMCN), Université catholique de Louivain, 1348 Louvain-la-Neuve, Belgium*

DISCUSSION 1: SUPERCELL APPROACH VS. VIRTUAL-CRYSTAL APPROXIMATION

We compare the supercell approach based on the use of SQSs and the virtual-crystal approximation (VCA) for the simulation of the optical properties of Ag-Au and Ag-Cu solid solutions by considering different atomic concentrations x and we show that, even in isoelectronic systems, the VCA does not in general predict the correct trends in metallic alloys.

In Ag-Au the qualitative behaviour and trends of the VCA and SQS optical absorption and reflectivity are very similar for all compositions considered (see Supplementary Figure 1). In both methods we observe a gradual shift of the onset of absorption in $\varepsilon_2(\omega)$ to higher energies by increasing the Ag content in Au, to which corresponds a gradual shift of the reflectivity edge. Indeed, the d bands lower gradually with respect to the Fermi level by increasing the concentration of Ag. The good agreement between SQS and VCA results is explained by the fact that the weak-scattering limit (see for example Ref. [8]) is a reasonable approximation for the isoelectronic Ag-Au system (and similarly for Au-Cu) and the electronic structure of the alloy can be considered as a mixture of the electronic structure of the single constituents. There is however a small discrepancy between the two approaches, given that a small lowering of the reflectivity in the low-energy part of the spectrum with respect to the pure elements is observed in the SQS simulations but not in the VCA simulations. This lowering of the reflectivity is experimentally measured in Ag-Au [9, 10] and it is actually a general effect observed in metallic alloys. It is due to the fact that the scattering of the conduction electrons in alloys is increased with respect to pure elemental crystals because of disorder.

Analogously to Ag-Au, in Supplementary Figure 2 we compare SQS and VCA simulations for the Ag-Cu system at different compositions. SQS results for Ag-Cu at relatively small Cu concentrations ($x = 0.25$) show a broad absorption peak centred at around 2.4 eV, i.e. below the absorption edge of elemental Ag, that is due to Cu impurity states and that is found also in the experimental data for Ag-Cu solid solutions [11] (see main text of the paper). For higher Cu concentrations ($x = 0.50$ and $x = 0.75$) the broad peak moves to lower energies and gradually deforms into the absorption edge of elemental Cu. In terms of reflectivity, this trend roughly corresponds to a shift of the reflectivity edge to lower frequencies and to a smoothening of the reflectivity edge by increasing the Cu content in Ag.

On the other hand, in VCA simulations, we observe a simple gradual shift of the onset of absorption to lower energies by varying the concentration of the alloy from elemental Ag to elemental Cu, which is very similar to the situation encountered in VCA simulations for the Ag-Au system. Because of this behaviour of the optical absorption, there is a corresponding simple gradual shift of the reflectivity edge to lower energies by increasing the Cu content in Ag. The broad absorption peak centered at around 2.4 eV for $x = 0.25$ is instead not observed in VCA simulations. Since the d bands of elemental Cu and Ag are more separated in energy, the weak-scattering limit in Ag-Cu is not as good as an approximation compared to Ag-Au and Au-Cu and thus the VCA method does not give the correct qualitative trends in optical properties compared to experiments for Ag-Cu solid solutions.

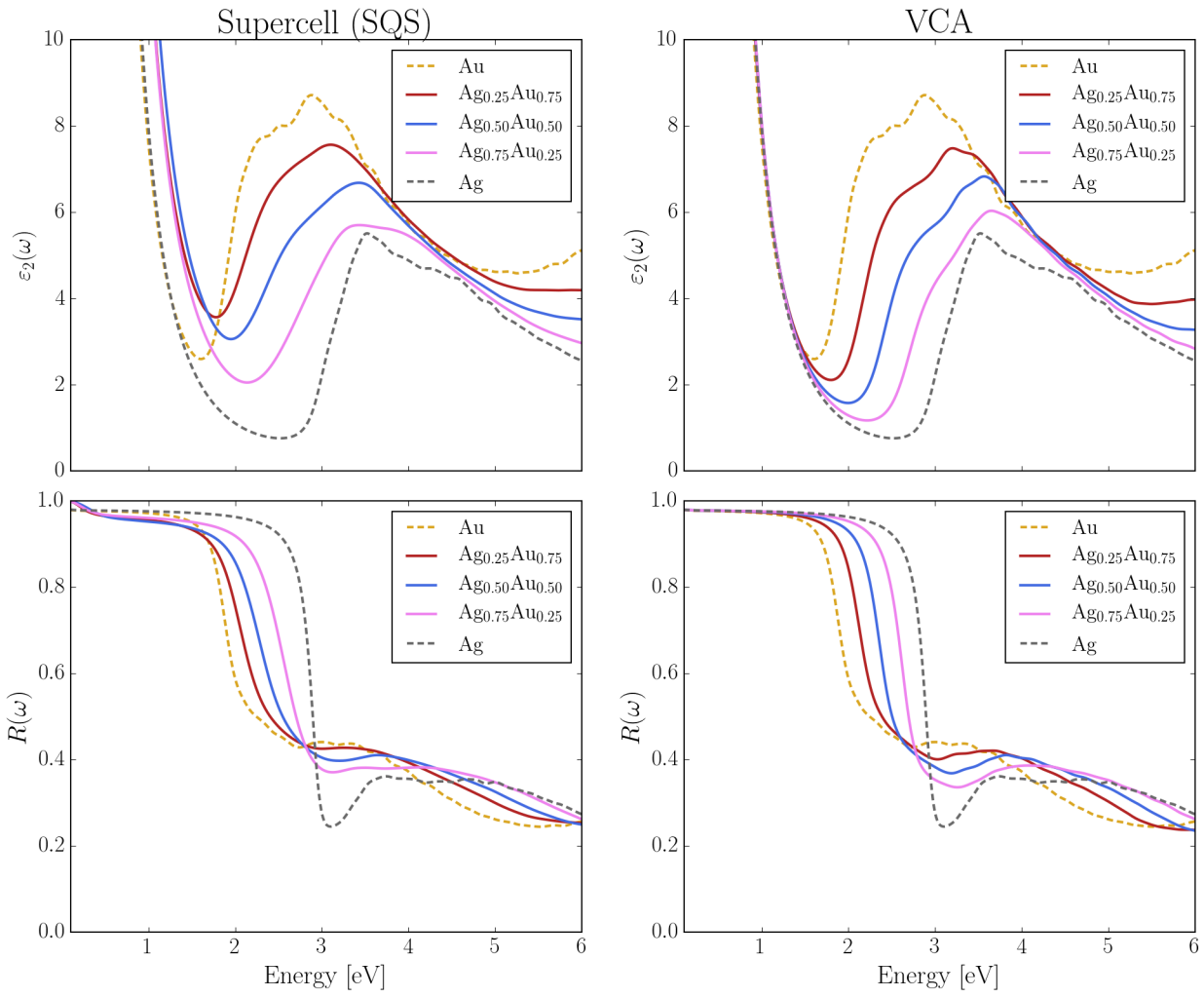

Figure 1: Comparison of the trends in composition of optical absorption and reflectivity for Ag-Au between SQS and VCA simulations. We report also the results for the elemental constituents, i.e. Ag and Au (dashed lines).

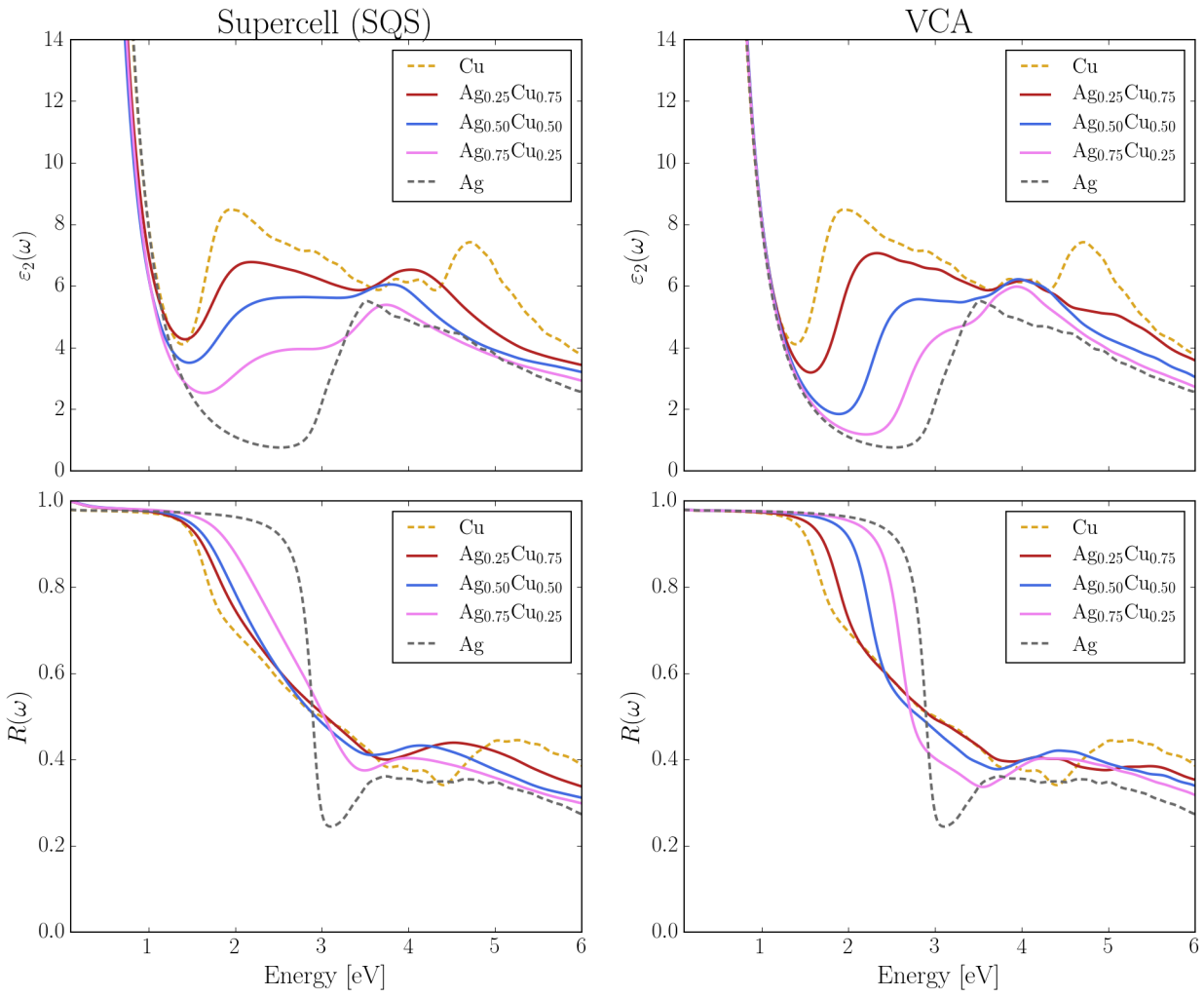

Figure 2: Comparison of the trends in composition of optical absorption and reflectivity for Ag-Cu between supercell and VCA simulations. We report also the results for the elemental constituents, i.e. Ag and Cu (dashed lines).

DISCUSSION 2: PSEUDOPOTENTIALS

Pseudopotentials and plane-waves cutoffs used for the evaluation of the IPA dielectric function are reported in Supplementary Table I, which shows all the relevant data for 55 elements of the periodic table. All pseudopotentials considered are norm-conserving because the `SIMPLE` code supports only this type of pseudopotentials. These are selected according to the results of the SSSP protocol to test pseudopotentials both in terms of precision and efficiency for several physically relevant quantities. However, for our purposes, we focus our attention only on the plane-wave convergence of band structure and on the precision of structural properties estimated through the Δ-factor test [1, 2]. In particular, the electronic band structures are a fundamental ingredient in the determination of the IPA dielectric function and thus, for our work, it is important to have well-converged band structures. By inspecting the data in the SSSP database of tests, we decide to use the SG15 (version 1.0 and 1.1) ONCV pseudopotential library for most of the elements of the periodic table because it is, in most of the cases, both precise and efficient. For each element, we select the converged plane-wave cutoffs to be used in our simulations such that each KS energy $E_{n\mathbf{k}}$ in the valence and in the conduction up to 10 eV above the Fermi level is converged at least within 20 meV (max η_{10} in Ref. [3]) for elemental solids. Since, in this work, we are mainly interested in the calculation of the optical properties within the visible range, the convergence of the band structure up to 10 eV above the Fermi level is a safe choice for a reliable estimation of the IPA dielectric function within this range. For a few problematic elements, i.e. Mn, Cr, Fe, Hf and Zn, we use the harder but more precise PseudoDojo (version 0.4) ONCV pseudopotentials.

We also verify that no ghost states up to 10 eV above the Fermi energy are present in the pseudopotentials selected.

Element	Pseudopotential	Cutoff [Ry]
Li	SG15 (1.0)	70
Be	SG15 (1.0)	60
B	SG15 (1.0)	55
C	SG15 (1.0)	80
N	SG15 (1.0)	80
Na	SG15 (1.0)	100
Mg	SG15 (1.0)	90
Al	SG15 (1.0)	80
Si	SG15 (1.1)	50
P	SG15 (1.1)	65
K	SG15 (1.0)	55
Ca	SG15 (1.0)	55
Sc	SG15 (1.0)	55
Ti	SG15 (1.0)	60
V	SG15 (1.0)	70
Cr	PseudoDojo (0.4)	100
Mn	PseudoDojo (0.4)	100
Fe	PseudoDojo (0.4)	100
Co	SG15 (1.0)	70
Ni	SG15 (1.0)	80
Cu	SG15 (1.0)	90
Zn	PseudoDojo (0.4)	90
Ga	SG15 (1.0)	90
Ge	SG15 (1.0)	70
As	SG15 (1.1)	50
Rb	SG15 (1.0)	50
Sr	SG15 (1.0)	55
Y	SG15 (1.0)	55
Zr	SG15 (1.0)	55
Nb	SG15 (1.0)	90
Mo	SG15 (1.0)	50
Tc	SG15 (1.0)	55
Ru	SG15 (1.0)	50
Rh	SG15 (1.0)	55
Pd	SG15 (1.0)	55
Ag	SG15 (1.0)	55
Cd	SG15 (1.0)	55
In	SG15 (1.1)	80
Sn	SG15 (1.1)	65
Sb	SG15 (1.1)	60
Te	SG15 (1.1)	55
Cs	SG15 (1.1)	60
Ba	SG15 (1.0)	60
Hf	PseudoDojo (0.4)	65
Ta	SG15 (1.0)	65
W	SG15 (1.0)	55
Re	SG15 (1.0)	90
Os	SG15 (1.0)	70
Ir	SG15 (1.0)	50
Pt	SG15 (1.0)	65
Au	SG15 (1.0)	55
Hg	SG15 (1.0)	65
Tl	SG15 (1.0)	60
Pb	SG15 (1.0)	50
Bi	SG15 (1.0)	50

Table I: List of pseudopotentials and corresponding plane-wave cutoffs chosen for 55 elements of the periodic table. We report in parenthesis the pseudopotential version.

DISCUSSION 3: SPIN-ORBIT COUPLING

All the calculations shown in the paper are performed at the scalar-relativistic level. Here we study the effect of spin-orbit coupling (SOC) on the optical properties of two heavy elements relevant for our work, i.e. gold and platinum (see Supplementary Figure 3).

In gold the largest relativistic effects come from the mass-velocity and the Darwin terms while SOC gives only a small correction [5]. In particular, the splitting of the bands induced by the SOC reduces the interband gap so that the absorption edge appears at a slightly lower energy. However, the shape of the reflectivity curve is not changed and the shift of the absorption edge leads, as a consequence, to a drop in the reflectivity curve a bit redshifted with respect to the scalar-relativistic calculation. Similarly, the SOC only reduces the IPA Drude plasma frequency by 0.2 eV (from 8.6 eV to 8.4 eV), given that the conduction band crossing the Fermi level is almost left unmodified by the inclusion of SOC [6]. However, because of the shift of the reflectivity edge, there is a perceivable change in colour between scalar-relativistic and fully relativistic simulations ($\Delta E = 3.6$). We notice that the correction in $R(\omega)$ due to the SOC is in the wrong direction compared to experiments and the simulated colour moves further way from the yellow part of the colour space (in terms of CIELAB colour space it means that b^* decreases).

In platinum the effect of SOC is more dramatic. The low-energy peak in $\varepsilon_2^{\text{inter}}(\omega)$ at 0.2 eV in the scalar-relativistic simulation due to *d*-*d* interband transitions is shifted by 0.6 eV to higher energies by including the SOC. This gives rise to a reduction in the reflectivity curve at around 0.8 eV that well reproduces the experimental data and that is absent in the scalar-relativistic case. The inclusion of SOC also reduces the Drude plasma frequency by nearly 20 % (from 8.4 eV to 7.2 eV). For platinum the effect of SOC is large but it modifies the optical properties in the infrared region of the spectrum and not in the visible so that the colour remains almost unchanged ($\Delta E = 1.0$). Besides, we note in passing that our results are in good agreement with previous all-electron calculations [5].

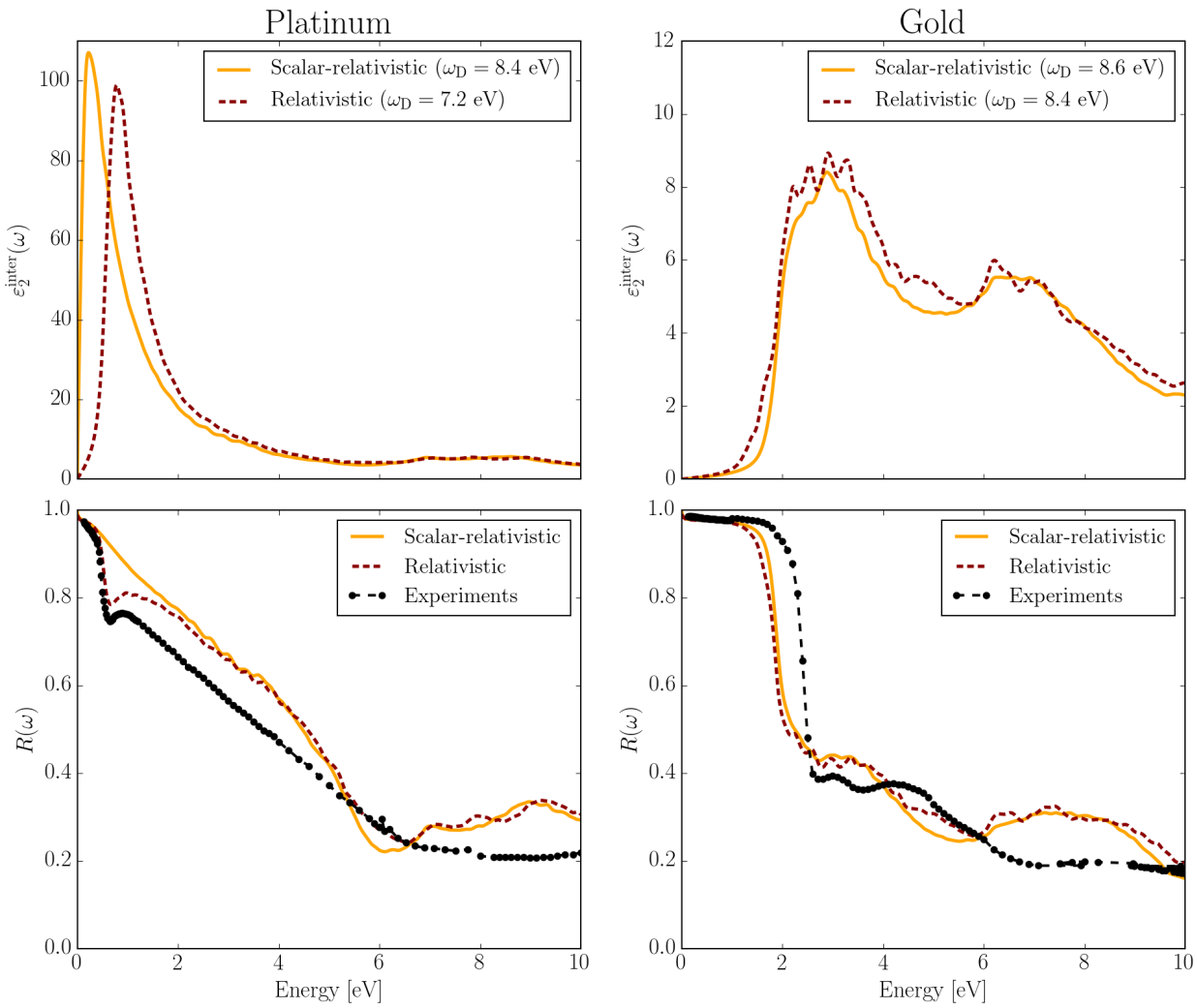

Figure 3: Comparison between the dielectric function and reflectivity for platinum and gold computed including ('Relativistic', dashed lines) and not including ('Scalar-relativistic', solid lines) SOC. Experimental data of the reflectivities (dot-dashed lines) are also reported [7].

* nicola.marzari@epfl.ch

[1] Lejaeghere, K. and Van Speybroeck, V. and Van Oost, G. and Cottenier, S. Error estimates for solid-state density-functional theory predictions: An overview by means of the ground-state elemental crystals. *Crit. Rev. Solid State Mater. Sci.* **39**, 1–24 (2014).

[2] Lejaeghere, K. *et al.* Reproducibility in density functional theory calculations of solids. *Science* **351**, aad3000 (2016).

[3] Prandini, G., Marrazzo, A., Castelli, I. E., Mounet, N. & Marzari, N. Precision and efficiency in solid-state pseudopotential calculations. *npj Comput. Mater.* **4**, 72 (2018).

[4] van Setten, M. *et al.* The pseudodojo: Training and grading a 85 element optimized norm-conserving pseudopotential table. *Comput. Phys. Commun.* **226**, 39 – 54 (2018).

[5] Glantschnig, K. & Ambrosch-Draxl, C. Relativistic effects on the linear optical properties of Au, Pt, Pb and W. *New J. Phys* **12**, 103048 (2010).

[6] Romaniello, P. & de Boeij, P. L. The role of relativity in the optical response of gold within the time-dependent current-density-functional theory. *J. Chem. Phys.* **122**, 164303 (2005).

[7] Palik, E. D. *Handbook of Optical Constants of Solids.* Academic Press handbook series (Elsevier Science, 1998).

[8] Ruban, A. V. & Abrikosov, I. A. Configurational thermodynamics of alloys from first principles: effective cluster interactions. *Rep. Prog. Phys.* **71**, 046501 (2008).

[9] Peña-Rodríguez, O. and Caro, M. and Rivera, A. and Olivares, J. and Manuel Perlado, J. and Caro, A. Optical properties of Au-Ag alloys: An ellipsometric study. *Opt. Mater. Express* **4**, 403–410 (2014).

[10] Nishijima, Y. & Akiyama, S. Unusual optical properties of the Au/Ag alloy at the matching mole fraction. *Opt. Mater. Express* **2**, 1226–1235 (2012).

[11] Rivory, J. Comparative study of the electronic structure of noble-metal-noble-metal alloys by optical spectroscopy. *Phys. Rev. B* **15**, 3119–3135 (1977).